J IRAN CHEM SOC
DOI 10.1007/s13738-016-0818-x

ORIGINAL PAPER

Nano-$CuFe_2O_4$-supported sulfonic acid as a novel and recyclable nanomagnetic acid for diazotization of aromatic amines: efficient synthesis of various azo dyes

Firouzeh Nemati[1] · **Ali Elhampour**[1] · **Mahshid B. Natanzi**[1] · **Samaneh Sabaqian**[1]

Received: 17 September 2015 / Accepted: 14 January 2016

Abstract A novel heterogeneous sulfonic acid functionalized nanomagnetic $CuFe_2O_4$ was successfully prepared and characterized by analyzing different obtained data including Fourier transform infrared spectroscopy, X-ray powder diffraction, field emission scanning electron microscopy, energy-dispersive X-ray spectroscopy, thermogravimetric analysis, dynamic light scattering and vibrating sample magnetometer. Then the novel acidic reagent was examined in synthesis of various azo-containing compounds from coupling of aryl diazonium ferrite sulfate salts with aromatic and non-aromatic compounds. The procedure starts by diazotization of aromatic amines with $NaNO_2$ and wet $CuFe_2O_4$–SO_3H and then coupling reaction of aryl diazonium ferrite sulfate salts with appropriate reagent. The prepared nano-solid acid showed high activity in synthesis of variety of aryl diazonium salts. In addition the as-prepared aryl diazonium ferrite sulfate salts are stable at room temperature for many hours and reacted efficiently in coupling reactions of aryl diazonium salts. All the azo dyes are synthesized in high yields and simple reaction conditions at room temperature. Moreover, the nanomagnetic solid acid was easily recovered from the reaction mixture and reused five runs without significant loss of activity.

Keywords Nanomagnetic-supported sulfonic acid · Diazonium salt · Azo dye · Aromatic amine

Introduction

Compounds containing azo groups linked to methine or aromatic-sp^2 hybridized-C atoms are the most important group of pharmaceutically important materials in the literature [1]. These compounds have received much attention and have wildly used in many practical applications such as coloring fiber, photoelectronic applications, printing systems, optical storage technology and in analytical chemistry [2]. Many azo compounds have been applied as chromogenic reagents for the determination of several metal ions [3]. The synthesis of azo dyes is usually carried out at low temperature in two steps: diazotization of arylamines with sodium nitrite in the presence of aqueous Bronsted acid, followed by reaction with electron-rich compounds or enol-type coupling components. The former is an interesting type of compound since they potentially have several tautomeric forms in solution and solid state [4]. The main limitation of such synthetic processes is their environmental incompatibility. The acidic effluents produce permanent damage to the environment and disturb the ecological balance.

One of the most important aims of "green chemistry" is to find alternative catalysts or reagents being readily available, inexpensive, selective, recyclable and environmentally benign [5]. In this context, supported heterogeneous acid catalysts have been actively investigated instead of harmful homogeneous acids such as H_2SO_4, HF, and H_3PO_4 [6].

Recently, magnetic nanoparticles have increasingly attracted interest as a support, due to their lack of toxicity, high thermal and mechanical stability, and adaptability for large-scale production and low price [7]. Remarkably, magnetic separation of the magnetic nanoparticles is more efficient than conventional filtration, simple, effective and economical and industrial applications. Among their various

✉ Firouzeh Nemati
fnemati_1350@yahoo.com; fnemati@semnan.ac.ir

[1] Department of Chemistry, Semnan University, Semnan 35131-19111, Iran

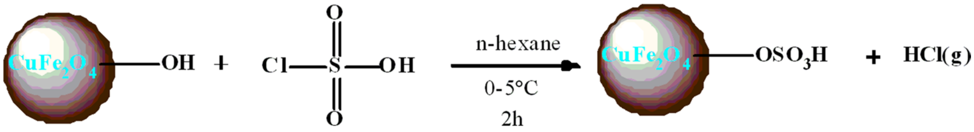

Scheme 1 Preparation of $CuFe_2O_4$–SO_3H nanoparticles

magnetic nanoparticles, mixed metal oxide nanoparticles became the strong candidates in the past few years and the improvements of modern organic synthesis are followed [8–10]. Hence, because of high catalytic activity of mixed metal oxide nanoscale, they are preferable than individual component oxides in diverse reactions [11, 12]. To this end, nanoscale copper ferrite particles are of great interest as a result of their efficient recycling, high stability, cleaning reaction profile and unique magnetic property [13].

Aryl diazonium salts are important intermediates that can be readily converted into a diverse functionality group [14]. High activity of diazonium group ($–N_2^+$) cases aryl diazonium salts possess sufficient potential energy to react spontaneously with generally low transition state barriers [15]. However, the key factors in the operation of such transformations are the easy availability, stability and safety of diazonium salts. So many researchers have investigated how to use them in a safer and more sustainable ways [16].

Therefore, considering the points above and in continuation of our studies in design of heterogeneous nanocatalysts [17–19] and successful attempt for the stabilization of aryl diazonium salts [20, 21], the aim of this work is to report the preparation and characterization of novel magnetic nano-acid, a superior heterogeneous acid, in the synthesis of aryl diazonium ferrite sulfate salts. Then the diazonium salts, $ArN_2^+ \, {}^-OSO_3CuFe_2O_4$, as stable precursors were used for the efficient synthesis of various azo compounds from diazo coupling of aryl diazonium ferrite sulfate salts with active aromatic and non-aromatic compounds under solvent-free grinding condition (Scheme 1).

Experimental

Preparation of nano-$CuFe_2O_4$–SO_3H

Firstly, the nano-$CuFe_2O_4$ particles were prepared according to literature report [22]. Then, in a flask, equipped with a constant-pressure dropping funnel and a gas inlet tube for conducting HCl gas over an adsorbing solution, nano-$CuFe_2O_4$ (1 g) was charged. Then, neat chlorosulfonic acid (3.3 mmol) was added drop-wise over a period of 0.5 h at 0–5 °C. HCl gas immediately evolved from the reaction vessel. After that, the mixture was shaken for 1 h at room temperature and nano-$CuFe_2O_4$–SO_3H was collected as a brown solid (1.25 g).

Loading of H^+

The loading of H^+ for the acidic magnetic nanoparticles was determined using potentiometric titration and it found to be 2.5 mmol/g.

General procedure for synthesis of aryldiazoium ferrite sulfate salts

An aromatic amin (1 mmol), nano-$CuFe_2O_4$–SO_3H (0.8 g) and a few drops of water (0.2 mL) ground in a mortar with a pestle to afford a homogeneous mixture, then $NaNO_2$ (2 mmol) was added. The reaction mixture was ground smoothly for 5–10 min. During this time the starting amine was consumed that was established by TLC monitoring.

General procedure for synthesis of azo compounds

The as-synthesized aryl diazonium salt was added to active compound (1 mmol) and the mixture was ground at room temperature for appropriate time; the color of the reaction will change [for the preparation of salt of 2-hydroxynaphthalene-1,4-dione and naphthol, we mixed 1 mmol from the former compounds with 0.8 mL water and NaOH (0.1 g, 2.5 mmol) in the other vessel and then added to the aryl diazonium salts]. After completion of the reaction (TLC), the mixture was washed by distilled water (50 mL) and the nano-$CuFe_2O_4$–SO_3H was separated using an external magnet. The solid products were filtrate and washed with EtOH. The most of the product were recrystallized from appropriate solvents and gave corresponding products in high yields. Some of them need purification with short column chromatography.

CAUTION! Although aryldiazoium ferrite sulfate salts are stable in the dry state, and we did not experience any problems, the operation needs to be conducted carefully, especially when they are subjected to grinding.

Spectroscopic data and physical properties of some selected compounds:

N,*N*-Dimethyl-4-[(2-nitrophenyl)diazenyl]aniline (**8a**) ^1H NMR (400 MHz, $CDCl_3$) δ: 17.90 (d, 2H, $J = 9.2$ Hz); 7.87 (d, d, 1H, $J = 4$ Hz, $J = 1.2$ Hz); 7.74 (d, d, 1H, $J = 4$ Hz, $J = 1.2$ Hz); 7.64 (t, d, 1H, $J = 4$ Hz, $J = 1.2$ Hz); 7.47 (t, d, 1H, $J = 4$ Hz, $J = 1.2$ Hz); 6.76 (d, 2H, $J = 9.2$ Hz); 3.14 (s, 6H, Me);

1-(Phenyldiazenyl)naphthalen-2-ol (**10a**): 1H NMR (400 MHz, $CDCl_3$) δ: 16.31 (s, 1H); 8.59 (d, 1H, $J = 8.4$ Hz,); 7.8 (s, 1H,); 7.6 (s, 1H,); 7.4 (s, 1H); 7.64–7.57 (m, 2H); 8.59 (t, 2H, $J = 7.52$ Hz); 7.43 (t, d, 1H, $J = 7.6$ Hz, $J = 1.2$ Hz); 7.34 (t, 1H, $J = 7.6$ Hz); 6.9 (d, 1H, $J = 9.2$);

2-[(4-Nitrophenyl)diazenyl]malononitrile (**2b**): bright red color; UV–Vis (DMSO) λmax1 (π–π*):478 nm; FTIR (KBr, cm^{-1}): υ 3222, 2229, 1598, 1342, 1510; ^1H NMR (400 MHz, DMSO): δ 8.25 (2H, d, $J = 9.2$ Hz), 7.61 (2H, d, $J = 9.2$ Hz), ^{13}C NMR (100 MHz, DMSO): δ 88.9; 109.8, 114.2, 117.1, 125.9, 144.3, 147.1; Anal. Calcd for $C_9H_5N_5O_2$: C, 50.23; H, 2.32; N, 32.55; found: C, 50.12; H, 2.45; N, 32.41.

Ethyl 2-cyano-2-(4-nitrophenyl)acetate (**5b**): yellow color; UV–Vis (DMSO) λmax1 (π–π*):494 nm; FTIR (KBr, cm^{-1}): υ 3215, 2200, 1699; ^1H NMR (400 MHz, DMSO): δ 12.61 (0.52 H, s), 8.30 (2H, t, $J = 8.8$ Hz), 7.76–7.64 (2H, m), 4.33 (2H, q, $J = 7.2$ Hz), 1.31 (3H, t, $J = 7.2$ Hz); ^{13}C NMR (100 MHz, DMSO): δ 14.56, 62.50, 108.22, 111.33, 116.56, 126.11, 143.75, 160.70; Anal. Calcd for $C_{11}H_{10}N_4O_4$: C, 50.38; H, 3.81; N, 21.37; found: C, 50.22, H, 3.65; N, 21.26.

2-[(4-Chlorophenyl)diazenyl]cyclohexane-1,3-dione (**8b**) brown color; UV–Vis (DMSO) λmax1 (π–π*):387 nm; ^1H NMR (400 MHz, DMSO): δ 7.48 (2H, d, $J = 8.8$ Hz), 7.387(2H, d, $J = 8.8$ Hz), 2.60 (4H, s), 1.13 (6H, s).

6-Amino-5-[(4-bromophenyl)diazenyl]-1,3-dimethylpyrimidine-2,4(1H,3H)-dione (**15b**) Orange color; UV–Vis (DMSO) λmax1 (π–π*):378 nm; ^1H NMR (400 MHz, DMSO): δ 10.27 (1H, s br), 9.63 (1H, s br), 7.46 (2H, d, $J = 7.2$ Hz), 7.10(2H, d, $J = 7$ Hz), 3.4 (3H, s), 3.2 (3H, s).

2-Hydroxy-3-(p-tolyldiazenyl)naphthalene-1,4-dione (**17b**) red color; UV–Vis (DMSO) λmax1 (π–π*):429 nm; FTIR (KBr, cm^{-1}): υ 3600–3200 (br), 1697; ^1H NMR (400 MHz, DMSO): δ 8.21 (1H, d, $J = 7.6$ Hz), 8.1 (1H, d of d, $J = 7.4$ Hz, $J = 0.8$ Hz), 7.96–7.85 (2H, m), 7.67 (2H, d, $J = 8$ Hz), 7.33 (2H, d, $J = 8.4$ Hz), 2.35 (3H, S); ^{13}C NMR (100 MHz, DMSO): δ 21.16, 118.29, 127.47, 130.79, 134.53, 135.46, 137.80, 139.51, 175.73; Anal. Calcd for $C_{17}H_{12}N_2O_3$: C, 69.86; H, 4.10; N, 9.58; found: C, 69. 71; H, 4.29; N, 9.41.

2-[(4-Chlorophenyl)diazenyl]-3-hydroxynaphthalene-1,4-dione (**18b**) red color; UV–Vis (DMSO) λmax1 (π–π*):379 nm; FTIR (KBr, cm^{-1}): υ 3600–3200 (br), 1699;^1H NMR (400 MHz, DMSO): δ 14.98 (0.23 H, s, br), 14.83 (0.23 H, s br), 8.23–8.12 (m, 2H), 7.99–7.80 (m, 4H), 7.60 (2H, d, $J = 8.4$ Hz); ^{13}C NMR (100 MHz, DMSO): δ 79.66, 119.66, 127.52, 128.13, 130.23, 131.32, 131.49, 133.65, 134.03, 134.43, 134.83, 135.16, 135.36, 135.49, 140.90, 141.07, 175.82, 179.29, 179.58, 181.85; Calcd for $C_{16}H_9N_2O_3Cl$: C, 61.44; H, 2.88; N, 8.96; found: C, 61.04, H, 2.92; N, 8.76.

Results and discussion

Characterization of nano-$CuFe_2O_4$–SO_3H

FT-IR and UV spectra

The infrared spectra of $CuFe_2O_4$ and $CuFe_2O_4$–SO_3H are depicted in Fig. 1. In Fig. 1a the band observed at 574 cm^{-1} indicated the Fe–O stretching vibration [23]. The characteristics peaks from the OSO_3H group of chlorosulfonic acid were observed at 3300, 1581, 1288 and 1064 cm^{-1} that corresponding to O–H, S=O and S–O groups, which clearly indicates the presence of –OSO_3H group over magnetic surface [24].The absorption spectra of $CuFe_2O_4$ and $CuFe_2O_4$–SO_3H in comparison with the unprotonated indicator (4-nitroaniline) are presented in Fig. 2, which confirms the presence of SO_3H groups and acidity strength of magnetic nano-$CuFe_2O_4$–SO_3H [25].

FE-SEM, EDX and DLS analysis

FE-SEM images of $CuFe_2O_4$ and $CuFe_2O_4$–SO_3H are shown in Fig. 3, which shows uniform-sized magnetic nanoparticles with somewhat spherical morphology and it has marked tendency to form large clusters. The nanoparticles that almost entirely separable from each other are apparent. It can be observed that there is no change in the shape of $CuFe_2O_4$ MNPs after being functionalized with sulfonic acid and the surface morphology is also retained (Fig. 3c). The elemental compositions of the $CuFe_2O_4$ from EDX

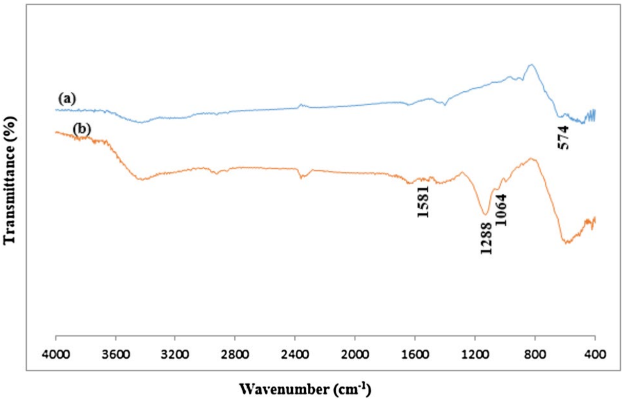

Fig. 1 The FTIR spectra of **a** nano-$CuFe_2O_4$ and **b** nano-$CuFe_2O_4$–SO_3H

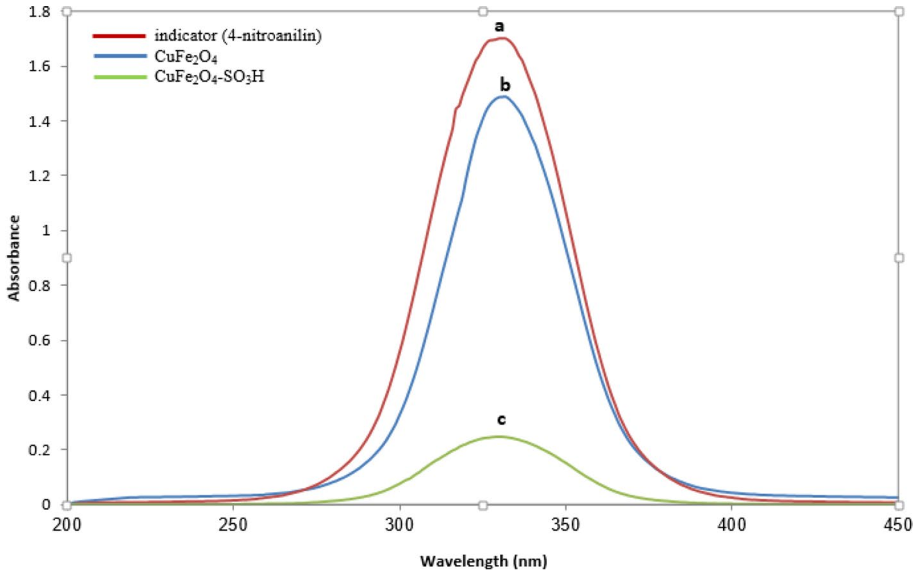

Fig. 2 Absorption spectra of **a** indicator **b** nano-$CuFe_2O_4$ and **c** nano-$CuFe_2O_4$–SO_3H

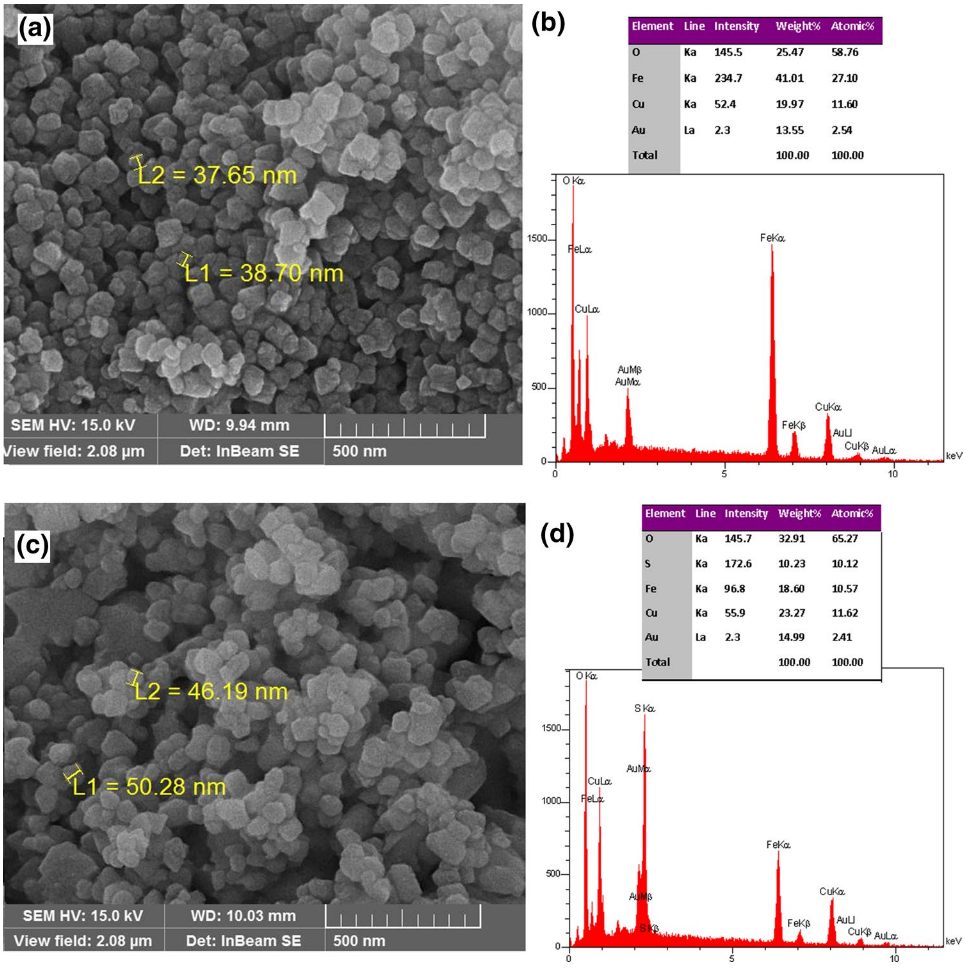

(b)

Element	Line	Intensity	Weight%	Atomic%
O	Ka	145.5	25.47	58.76
Fe	Ka	234.7	41.01	27.10
Cu	Ka	52.4	19.97	11.60
Au	La	2.3	13.55	2.54
Total			100.00	100.00

(d)

Element	Line	Intensity	Weight%	Atomic%
O	Ka	145.7	32.91	65.27
S	Ka	172.6	10.23	10.12
Fe	Ka	96.8	18.60	10.57
Cu	Ka	55.9	23.27	11.62
Au	La	2.3	14.99	2.41
Total			100.00	100.00

Fig. 3 The FEG-SEM–EDS analysis of **a**, **b** nano-$CuFe_2O_4$ and **c**, **d** nano-$CuFe_2O_4$–SO_3H

analysis also exhibited in Fig. 2b and show the presence of Cu, Fe and O elements. The presence of sulfur peak in addition of Cu, Fe and O in Fig. 2d, clearly indicate the successful functionalization of $CuFe_2O_4$. According to DLS results the size distribution of particles were significantly narrow (Fig. 4).

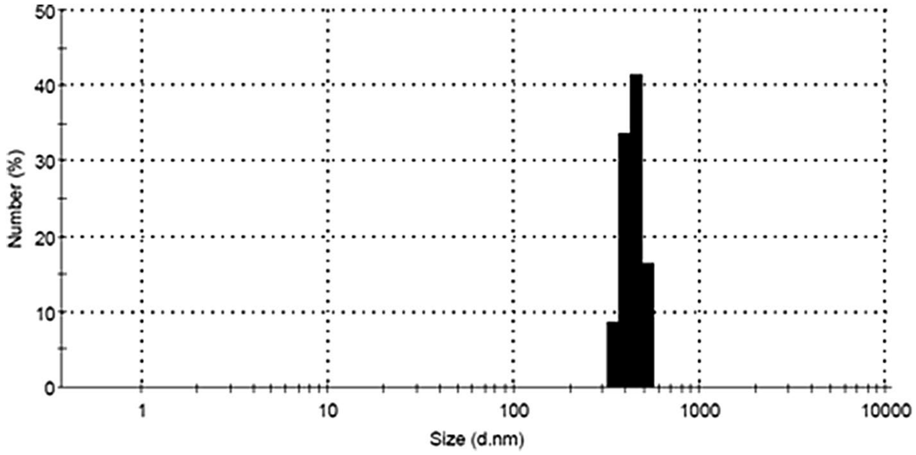

Fig. 4 Distribution of hydrodynamic diameter for the nano-$CuFe_2O_4$

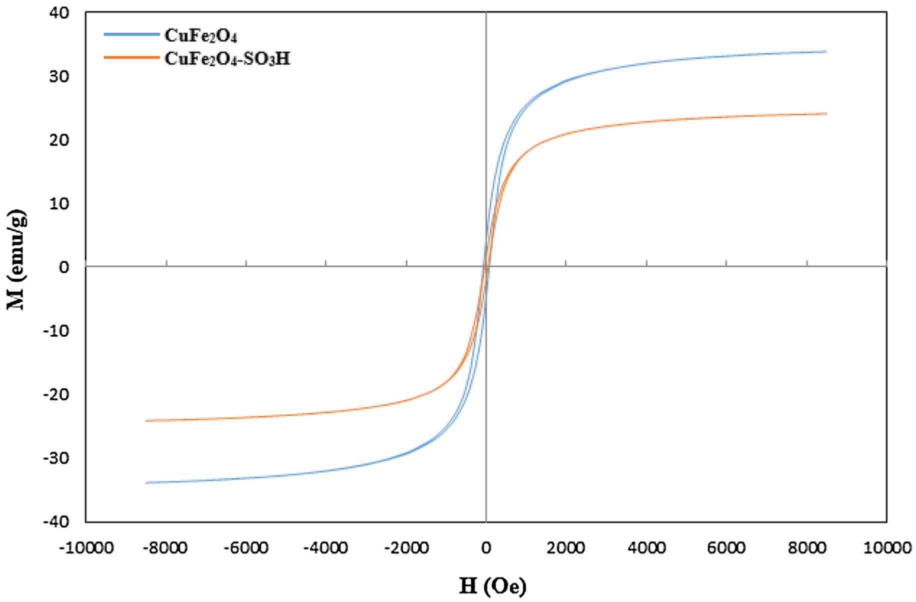

Fig. 5 The magnetization curves of nano-$CuFe_2O_4$ and nano-$CuFe_2O_4$–SO_3H

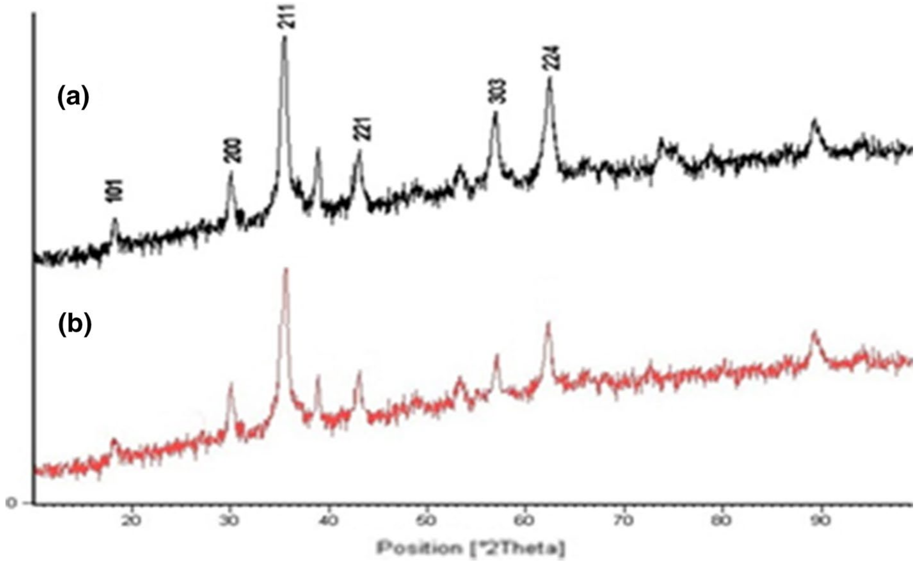

Fig. 6 XRD patterns of **a** nano-$CuFe_2O_4$ and **b** nano-$CuFe_2O_4$–SO_3H

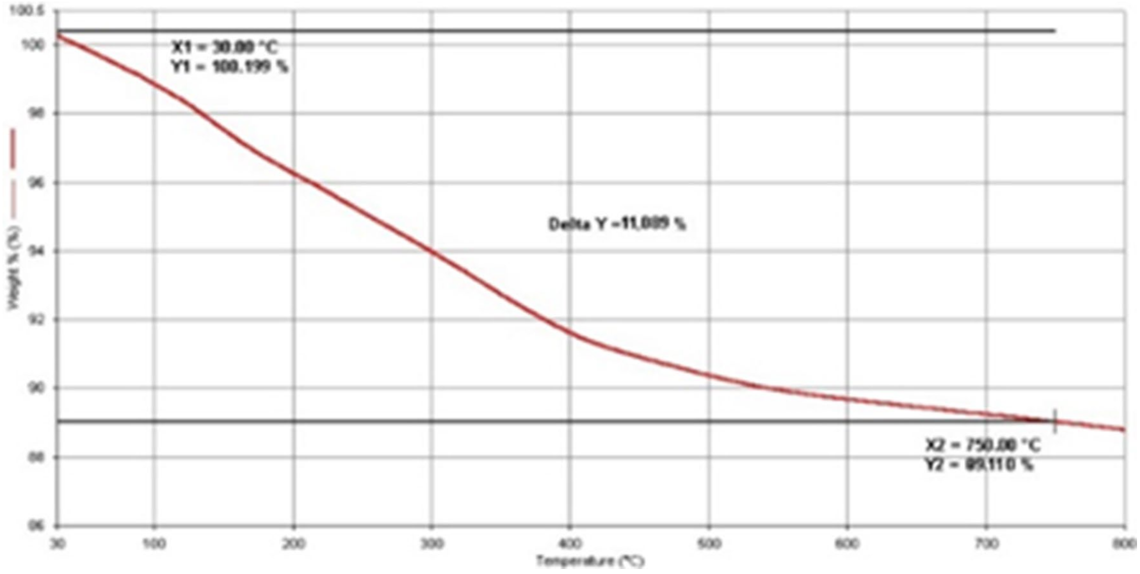

Fig. 7 TGA of nano-$CuFe_2O_4$–SO_3H

VSM analysis

The saturation magnetization of $CuFe_2O_4$ and $CuFe_2O_4$–SO_3H was 33.85 and 24.11 emu/g, respectively. Obviously, after the preparation of $CuFe_2O_4$–SO_3H, its magnetic response was affected due to coating with non-magnetic materials [26] (Fig. 5). Nonetheless, this magnetic property is enough and the $CuFe_2O_4$–SO_3H could be completely and quickly separated from the reaction mixture when an external magnetic force was applied.

X-ray diffraction spectrum (XRD)

The XRD spectrum of $CuFe_2O_4$ clearly matches well with the literature data (Fig. 6). Six peaks at 18.3, 30.3, 35.6, 42.8, 57.1 and 62.98 can be assigned to the (101), (200), (211), (221), (303) and (224) diffraction peaks of $CuFe_2O_4$ spinel, respectively (Fig. 6a) [27]. Notably, the same peaks were also observed in $CuFe_2O_4$–SO_3H XRD spectra, which indicate the structural stability of $CuFe_2O_4$ with SO_3H modification. The crystallite size of the nanoparticles was calculated to be around 29 nm from the XRD results using the Debye–Scherrer equation.

Thermo-gravimetric analyses (TGA)

The thermal stability of the $CuFe_2O_4$–SO_3H was observed by TG analysis (Fig. 7). In the TG curve of acidic MNPs, the first weight loss below 150 °C is due to remove of trapped solvent molecules from the lattice. Another weight loss of approximately 9 % beginning from 150 up to 700 °C can be attributed to the decomposition of sulfonic acid groups from the $CuFe_2O_4$ surface. Thus, the catalyst was stable sufficiently and could be used in organic reactions at elevated temperatures.

Preparation of stable aryl diazonium ferrite sulfate salts

After the successful characterization of heterogeneous magnetic acid, the acid activity of $CuFe_2O_4$–SO_3H was examined for its ability to produce the stable aryl diazonium ferrite sulfate salts from aromatic amines. In order to optimize the amount of solid acid, different quantity of $CuFe_2O_4$–SO_3H used to confirm its effects in prepare of diazonium salts. As shown in Scheme 2, a mixture of 4-nitroaniline (1 mmol), $CuFe_2O_4$–SO_3H (0.8 g), water (0.2 mL) and

Scheme 2 The model reaction for optimization of synthesis of stable aryldiazonium ferrite sulfate salt

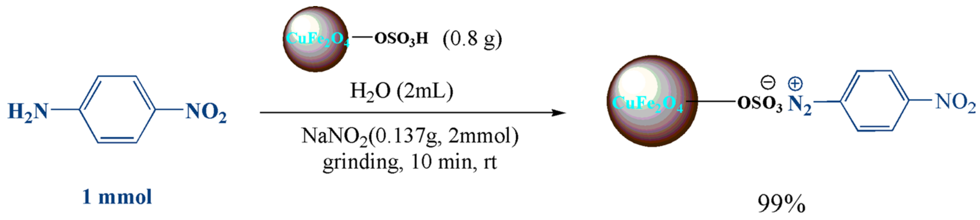

sodium nitrite (2 mmol) in grinding condition, gave an excellent yield of stable 4-nitro benzene diazonium ferrite sulfate salt (99 %) at room temperature (Scheme 2).

Coupling of stable aryl diazonium ferrite sulfate salts with active compounds: synthesis of azo dyes

Coupling with active aromatic compounds

The reaction of stable aryl diazonium ferrite sulfate salts with a number of active aromatic compounds was investigated and results depicted in Table 1. All the reactions were carried out under solvent-free condition at room temperature in mild and heterogeneous conditions. The corresponding azo dyes were obtained in good to high yields. The reactions were completed within 10–15 min, with good isolated yields. Aryl diazonium ferrite sulfate salts with electron-withdrawing groups or electron-donating groups also reacted effectively. The Steric effects of *ortho* substituents had little influence on the yields and reaction times. In addition, it was observed that the reaction of phenolic compounds have higher yields in basic media. The diazonium salts with an electron-withdrawing substituent provided better results in comparison to those having electron-donating substituent.

Coupling with active non-aromatic compounds

After the successful synthesis of azo dyes from the reaction of stable aryl diazonium ferrite sulfate salts with active aromatic compounds, we decided to investigate the efficiency of coupling of these diazonium salts with non-aromatic active compounds. For this purpose, a

Table 1 Condensation of aryl diazonium ferrite sulfate salts with various active aromatic compounds

Entry	G	Active aromatic compounds	Product	Yield %	Mp (Lit) °C	Color
1	H	*N*,*N*-Dimethylaniline	**1a**	82	110–113 [28]	Yellow
2	*p*-NO_2	*N*,*N*-Dimethylaniline	**2a**	95	218–220 [29]	Deeply colored
3	*p*-Et	Phenol	**3a**	75	270 [29]	Yellow
4	*p*-NO_2	Phenol	**4a**	90	207–210 [29]	Brown
5	*p*-SO_3H	*N*,*N*-Dimethylaniline	**5a**	90	300–303 [30]	Brown
6	*p*-Cl	*β*-Naphthol	**6a**	85	75 [31]	Red
7	*o*-NO_2	*β*-Naphthol	**7a**	83	280–282 [32]	Orange
8	*o*-NO_2	*N*,*N*-Dimethylaniline	**8a**	85	130–132 [29]	Orange
9	*p*-NO_2	Aniline	**9a**	85	198–203 [33]	Orange
10	H	*β*-Naphthol	**10a**	87	130–131 [29]	Red
11	*p*-Cl	Phenol	**11a**	82	188–190 [34]	Black

Table 2 Condensation of aryl diazonium ferrite sulfate salts with non-aromatic active compounds

Entry	G	Active methylene compounds	Product	Yield %	Mp (Lit) °C	Color
1	H	Malononitrile	**1b**	92	136–138 [36]	Red
2	*p*-NO_2	Malononitrile	**2b**	99	141–143	Yellow
3	*p*-Cl	Malononitrile	**3b**	95	184.5–186 [36]	Yellow
4	*m*-Cl	Malononitrile	**4b**	85	170–173 (dec.) [37]	Yellow
5	*p*-NO_2	Ethyl cyanoacetate	**5b**	98	179–180	Yellow
6	*p*-NO_2	Dimedone	**6b**	90	157–158 [38]	Red
7	*m*-NO_2	Dimedone	**7b**	80	124–125 [38]	Yellow
8	*p*-Cl	Dimedone	**8b**	87	216–219 [38]	Brown
9	H	Dimedone	**9b**	85	119 [40]	Yellow
10	H	Barbituric acid	**10b**	80	317–318.5 (dec.) [39]	Orange
11	*p*-Me	Barbituric acid	**11b**	88	194–196 [40]	Yellow
12	*p*-Br	Barbituric acid	**12b**	75	245–248 [41]	Yellow
13	*p*-NO_2	Uracil	**13b**	77	310–313 [42]	Orange
14	*p*-Me	Uracil	**14b**	75	259.7–261.7 [42]	Yellow
15	*p*-Br	Uracil	**15b**	78	238–239	Yellow
16	2-Pyridine	Uracil	**16b**	73	258–259 [42]	Red
17	*p*-Me	2-Hydroxy quinoline	**17b**	75	237–237.5	Red
18	*p*-Cl	2-Hydroxy quinoline	**18b**	80	208–209	Red

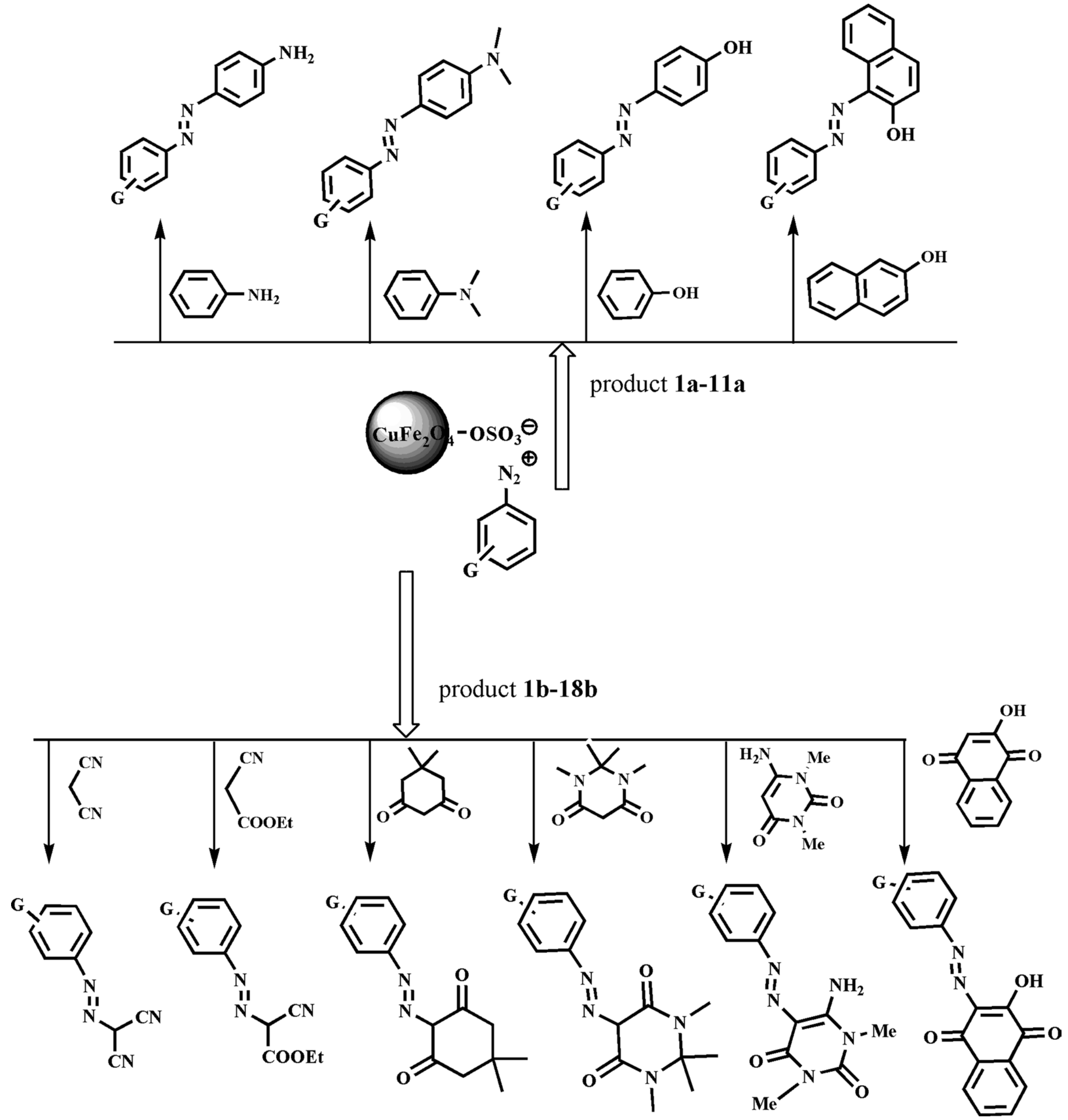

Scheme 3 Synthesis various azo dyes using nano-$CuFe_2O_4$–SO_3H

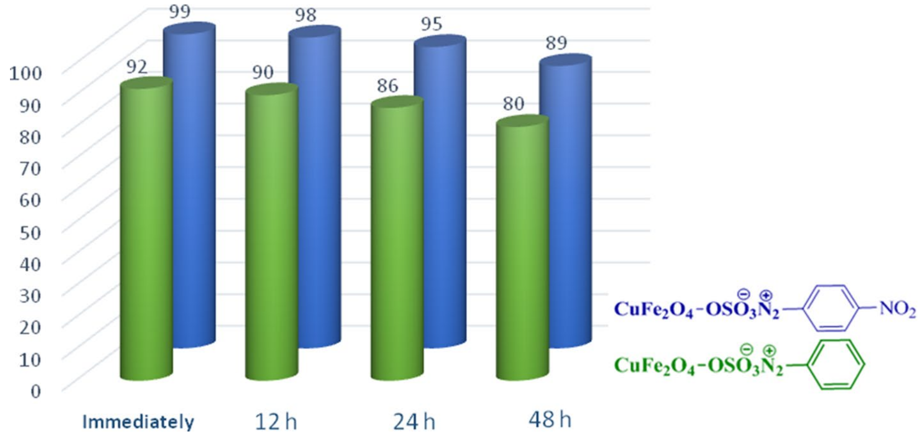

Fig. 8 The stability of aryl diazonium ferrite sulfate salts at room temperature (reaction condition: aryl diazonium ferrite sulfate salts, malononitrile)

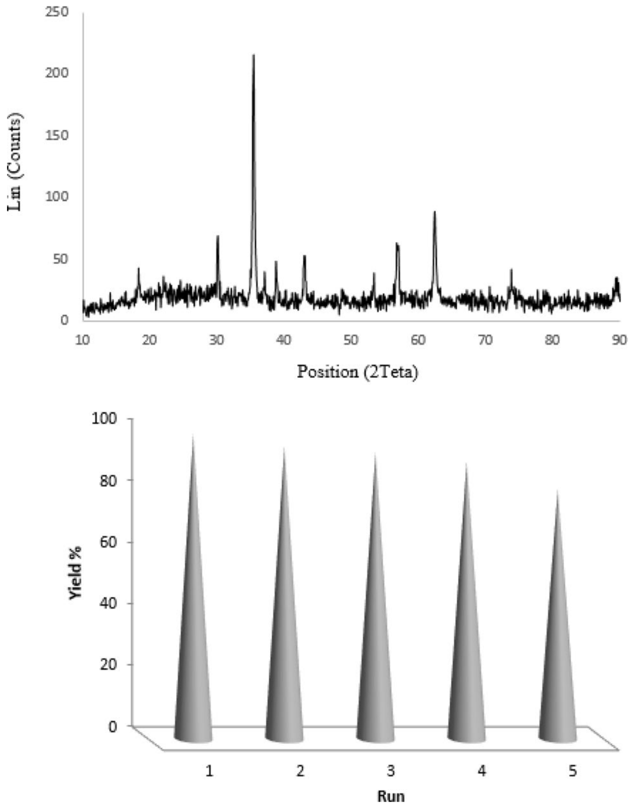

Fig. 9 Recyclability of $CuFe_2O_4–SO_3H$ after four runs

series of active non-aromatic compounds involves dimedone, barbituric acid, uracil, malononitrile, 2-hydroxy quinoline and ethyl cyanoacetate were selected and the coupling reaction of stable aryl diazonium ferrite sulfate salts were examined. We mixed the diazonium salt and active compounds in stochiometric amounts in a mortar and ground the mixture with the help of a pestle until the completion of the reaction. The corresponding results are summarized in Table 2. As it can be seen in Table 2, our method was highly efficient and general in the synthesis of diverse azo compounds; a series of active non-aromatic compounds including malononitrile, ethyl cyanoacetate, dimedone, barbituric acid and uracil coupled efficiently and the desired products were produced in high yields and purity (Scheme 3). Also the reaction times were short. Fortunately, the coupling of aryl diazonium ferrite sulfate salts with 2-hydroxynaphthalene-1,4-dione gave the corresponding azo compounds in excellent yields (**17e**, **18e**) that is different from previously reported procedure [35].

Stability of aryl diazonium ferrite sulfate

In an attempt to study the stability of aryl diazonium ferrite sulfate salts, the reaction of them with malononitrile was investigated after the times specified in Fig. 8. As shown in Fig. 8, the addition of malononitrile to the stored diazonium ferrite sulfate salts (they stored in a desiccator at room temperature) provided almost the same yield of product as that from freshly prepared salt. Obviously, because of the instability of aryl cation, the aryl diazonium salts with electron-withdrawing group has the higher stability [43].

Recycling of the nanomagnetic solid acid

To explore the extent of recyclability of our acidic nanomagnetic particles, its recyclability was tested by recycling of $CuFe_2O_4–SO_3H$ in the coupling reaction of malononitrile and 4-nitrophenyl diazonium ferrite sulfate. In each cycle the MNPs was separated magnetically and washed several times with water and ethylacetate to ensure the organic and inorganic reagents do not remain on the surface of magnetic nanoparticles. Then, the recovered MNPs reused in subsequent runs. It was found that the performance of MNPs retains for a minimum four reaction cycles and displayed almost high catalytic performance with over 89 % product yield. Moreover, the XRD pattern of recycled catalyst showed that the nano-$CuFe_2O_4–SO_3H$ was the similar to the initial one after four runs (Fig. 9).

Conclusions

In conclusion, we have prepared a new nanomagnetic solid acid catalyst via grafting of sulfonic acid groups on nano-$CuFe_2O_4$ magnetic particles. The catalyst is stable under air atmosphere and can readily be recovered by an external magnet field. This new heterogeneous catalyst showed many advantages including simple synthesis, easy magnetic separation, excellent reusability, high loading of H^+ and tolerability of a broad range of functional groups.

Acknowledgments The authors gratefully acknowledge Semnan University Research Council for financial support of this work.

References

1. A. Zarei, A.R. Hajipour, L. Khazdooz, B.F. Mirjalili, A.N. Chermahini, Dyes Pigments **81**, 240 (2009)
2. G. Kurtoglu, B. Avar, H. Zengin, M. Kose, K. Sayin, M. Kurtoglu, J. Mol. Liq. **200**, 105 (2014)
3. K. AL-Adilee, A. Ghali, A.S. Hussein, J. Chem. Eng **6**, 651 (2012)
4. E.O. Moradi, M. Rufchahi, J. Mol. Liq. **199**, 393 (2014)
5. M.B. Gawande, Y. Monga, R. Zboril, R.K. Sharma, Coord. Chem. Rev. **288**, 118 (2015)
6. I. Fechete, Y. Wang, J.C. Vedrin, Catal. Today **189**, 2 (2012)
7. Wang D. Astruc, Chem. Rev. **114**, 6949 (2014)
8. R. Narayanan, Green Chem. Lett. Rev. **5**, 707 (2012)
9. R.B.N. Baig, R.S. Varma, Green Chem. **15**, 398 (2013)

10. M.B. Gawande, V.D.B. Bonifácio, R.S. Varma, I.D. Nogueira, N. Bundaleski, C.A.A. Ghumman, O.M.N.D. Teodorod, P.S. Branco, Green Chem. **15**, 1226 (2013)
11. A. Kazaei, A. Ranjbaran, F. Abbasi, M. Khazaei, A.R. Mousavizare, RSC Adv. **5**, 13643 (2015)
12. E. Rafiee, S. Eavania, Green Chem. **13**, 2116 (2011)
13. A.S. Kumar, B. Thulasiram, S.B. Laxmi, V.S. Rawat, B. Sreedhar, Tetrahedron **70**, 6059 (2014)
14. L. He, G. Qiu, Y. Gao, J. Wu, Org. Biomol. Chem. **12**, 6965 (2014)
15. K.S. Nalivela, M. Tilley, M.A. McGuire, M.G. Organ, Chem. Eur. J. **20**, 6603 (2014)
16. N. Oger, E. Le Grognec, F.X. Felpin, Org. Chem. Front. **2**, 590 (2015)
17. F. Nemati, M.M. Heravi, A. Elhampour, RSC Adv. **5**, 45775 (2015)
18. F. Nemati, A. Elhampour, H. Farrokhi, M.B. Natanzi, Catal. Commun. **66**, 15 (2015)
19. F. Nemati, M.M. Heravi, R. Saeedirad, Chin. J. Catal. **33**, 1825 (2012)
20. F. Nemati, A. Elhampour Sci. Iran **19**, 1594 (2012)
21. F. Nemati, A. Elhampour, J. Chem. Sci. **124**, 889 (2012)
22. S.M. Baghbanian, M. Farhang, RSC Adv. **4**, 11624 (2014)
23. K. Pradhan, S. Paul, A.R. Das, Catal. Sci. Technol. **4**, 822 (2014)
24. M.B. Gawande, A.K. Rathi, I.D. Nogueira, R.S. Varma, P.S. Branco, Green Chem. **15**, 1895 (2013)
25. A. Amoozadeh, S. Rahmani, J. Mol. Catal. A **396**, 96 (2015)
26. N. Koukabi, E. Kolvari, M.A. Zolfigol, A. Khazaei, BSh Saghasemi, B. Fasahati, Adv. Synth. Catal. **354**, 2001 (2012)
27. Gh Imani Shakibaei, R. Ghahremanzadeh, A. Bazgir, Monatsh Chem. **145**, 1009 (2014)
28. H. Valizadeh, M. Amiri, A. Shomali, F. Hosseinzadeh, J. Iran. Chem. Soc. **8**, 495 (2011)
29. H. Valizadeh, A. Shomali, Dyes Pigments **92**, 1138 (2012)
30. Q. Zhang, S. Zhang, S. Liu, X. Ma, L. Lu, Y. Deng, Analyst **136**, 1302 (2011)
31. B.F. Mirjalili, A. Bamoniri, A. Akbari, Curr. Chem. Lett. **1**, 109 (2012)
32. M.J.D. Long, H.J. Prochaska, P. Talalay, Med. Sci. **83**, 787 (1989)
33. M.L. Rahman, C. Tschierske, M. Yusoff, S. Silong, Tetrahedron Lett. **46**, 2303 (2005)
34. O.O. Ajani, O.E. Akinremi, A.O. Ajani, A. Edobor-Osoh, W.U. Anake, Phys. Rev. Res. Int. **3**, 24 (2013)
35. J. Asselin, P. Brassard, P. L'ecuyer, Can. J. Chem. **44**, 2563 (1966)
36. P.C. Tsai, I.J. Wang, Dyes Pigments **64**, 259 (2005)
37. P.G. Heytler, W.W. Prichard, Biochem. Biophys. Res. Commun. **7**, 272 (1962)
38. M. George, M. Jolocam, B. Odongkara, H. Twinomuhwezi, G.B. Mpango, Res. J. Chem. Sci. **1**, 102 (2011)
39. N. Noroozi-pesyan, J. Khalafy, Z. Malekpoor, J. Chin. Chem. Soc. **2**, 61 (2009)
40. H.G. Garg, R.A. Sharma, J. Pharm. Sci. **59**, 1691 (1970)
41. G. Kaupp, A. Herrmann, J. Schmeyers, Chem. Eur. J. **8**, 1395 (2002)
42. M. Yazdanbakhsh, M. Abbasnia, M. Sheykhan, J. Mol. Struct. **977**, 266 (2010)
43. F. Mo, G. Dong, Y. Zhanga, J. Wang, Org. Biomol. Chem. **11**, 1582 (2013)